

Synthesis and Properties of Fuel Cell Anodes Based on $(\text{La}_{0.5+x}\text{Sr}_{0.5-x})_{1-y}\text{Mn}_{0.5}\text{Ti}_{0.5}\text{O}_{3-\delta}$ ($x = 0-0.25$, $y = 0-0.03$)¹

A. I. Ivanov^{a,z}, D. A. Agarkov^a, I. N. Burmistrov^a, E. A. Kudrenko^a,
S. I. Bredikhin^a, and V. V. Kharton^{a,b}

^a*Institute of Solid State Physics, ul. Akad. Osip'yana 2, Chernogolovka, Moscow Region, 142432 Russia*

^b*Department of Materials and Ceramic Engineering, CICECO, University of Aveiro, Portugal*

Received August 26, 2013

Abstract—Results are presented of studying electrochemical properties of perovskite-like solid solutions $(\text{La}_{0.5+x}\text{Sr}_{0.5-x})_{1-y}\text{Mn}_{0.5}\text{Ti}_{0.5}\text{O}_{3-\delta}$ ($x = 0-0.25$, $y = 0-0.03$) synthesized using the citrate technique and studied as oxide anodic materials for solid oxide fuel cells (SOFC). X-ray diffraction (XRD) analysis is used to establish that the materials are stable in a wide range of oxygen chemical potential, stable in the presence of 5 ppm H_2S in the range of intermediate temperatures, and also chemically compatible with the solid electrolyte of $\text{La}_{0.8}\text{Sr}_{0.2}\text{Ga}_{0.8}\text{Mg}_{0.15}\text{Co}_{0.05}\text{O}_{3-\delta}$ (LSGMC). It is shown that transition to a reducing atmosphere results in a decrease in electron conductivity that produced a significant effect on the electrochemical activity of porous electrodes. Model cells of planar SOFC on a supporting solid–electrolyte membrane (LSGMC) with anodes based on $(\text{La}_{0.6}\text{Sr}_{0.4})_{0.97}\text{Mn}_{0.5}\text{Ti}_{0.5}\text{O}_{3-\delta}$ and $(\text{La}_{0.75}\text{Sr}_{0.25})_{0.97}\text{Mn}_{0.5}\text{Ti}_{0.5}\text{O}_{3-\delta}$ and a cathode of $\text{Sm}_{0.5}\text{Sr}_{0.5}\text{CoO}_{3-\delta}$ are manufactured and tested using the voltammetry technique.

Keywords: solid oxide fuel cells, anode, perovskite, citrate synthesis, redox stability

DOI: 10.1134/S1023193514080047

INTRODUCTION

Perovskite-like oxygen–ion conductors based on lanthanum gallate are one of the most promising groups of solid electrolytes for solid–oxide fuel cells (SOFC) functioning at intermediate temperatures [1, 2]. Application of gallates in SOFC is, however, limited by the relatively high reactivity towards many electrode materials, including Ni–cermet anodes [3]. This regularity and degradation of nickel cermets in atmospheres containing hydrocarbon fuels and sulfur compounds [4, 5] at enhanced temperatures and at significant variation of chemical potential of oxygen in the gas phase cause a necessity of developing new anodic materials based on oxide compounds with mixed ion–electron conductivity. Such materials must have high electron and anion conductivity, high catalytic activity in the reactions of fuel oxidation, thermal expansion coefficients close to those of the other fuel cell materials, and thermodynamic stability both in the oxidative atmosphere in the course of SOFC manufacturing and in reducing atmospheres under the conditions of practical application. The above standard requirements are in part satisfied by the solid solutions of $(\text{La},\text{Sr})(\text{Cr},\text{Mn},\text{Ti})\text{O}_{3-\delta}$ with a perovskite ABO_3 structure, where A and B stand for metal cations

[6]. However, the presence of chromium in the *B*-sublattice of the perovskite structure may cause negative effects related to evaporation of chromium oxides at high temperatures and formation of Cr^{6+} during storage in air. Therefore, chromium–free compounds are of practical interest. For example, perovskite with the composition of $\text{La}_{0.4}\text{Sr}_{0.6}\text{Ti}_{0.8}\text{Mn}_{0.2}\text{O}_{3-\delta}$ was studied as an anodic material for SOFC with solid electrolyte membranes based on zirconia [7]. Some works [8–10] also showed the possible prospects for using lanthanum–strontium manganites–titanates as SOFC anodes.

This work was centered on synthesis of submicron powders of perovskite-like oxides of the system of $(\text{La}_{0.5+x}\text{Sr}_{0.5-x})_{1-y}\text{Mn}_{0.5}\text{Ti}_{0.5}\text{O}_{3-\delta}$ (LSTM) using the citrate technique. Stability of the obtained materials in reducing media containing small amounts of H_2S , reactivity towards the material of electrolyte, and specific conductivity in oxidative and reducing atmospheres were investigated. To estimate practical applicability, model SOFCs with anodes based on $(\text{La}_{0.5+x}\text{Sr}_{0.5-x})_{1-y}\text{Mn}_{0.5}\text{Ti}_{0.5}\text{O}_{3-\delta}$, where $\text{La}_{0.8}\text{Sr}_{0.2}\text{Ga}_{0.8}\text{Mg}_{0.15}\text{Co}_{0.05}\text{O}_{3-\delta}$ (LSGMC) was used as electrolyte, were manufactured and characterized. This electrolyte was chosen for the case studies, as introduction of 5% of cobalt into the *B*-sublattice of gallate might cause a significant increase in ionic conductivity [11]. Perovskite $\text{Sm}_{0.5}\text{Sr}_{0.5}\text{CoO}_{3-\delta}$ (SSC),

¹ This publication was prepared based on a lecture delivered at the All-Russian Conference with international participation “Fuel Cells and Power Plants,” Chernogolovka, 2013.

^z Corresponding author: aliv@issp.ac.ru (A.I. Ivanov).

also well known in the literature [12], was used for cathodes.

EXPERIMENTAL

Synthesis of $(\text{La}_{0.5+x}\text{Sr}_{0.5-x})_{1-y}\text{Mn}_{0.5}\text{Ti}_{0.5}\text{O}_{3-\delta}$ ($x = 0-0.25$, $y = 0-0.03$) was carried out using the citrate technique according to the Pechini modification [13]. The initial compounds used were: $\text{La}(\text{NO}_3)_3 \cdot 6\text{H}_2\text{O}$ (reagent grade), $\text{Sr}(\text{NO}_3)_2$ (analytical grade), $\text{Mn}(\text{CH}_3\text{COO})_2 \cdot 4\text{H}_2\text{O}$ (pure grade), TiO_2 (ultra high grade), and citric acid (pure). Metal salts were dissolved in distilled water with addition of citric acid under vigorous mixing on a magnetic stirrer until the medium was completely homogenized. Evaporation at 400 K was carried out until a viscous mass was formed, to which highly dispersed TiO_2 was added under vigorous mixing. After weakly bound water was fully removed, the sample was heated to ~ 570 K to initiate the combustion reaction. The obtained precursors were thoroughly ground in an agate mortar and sintered in air at 1073 K for 5 h. Then, the powders were ground in ethanol (a Fritsch planetary ball mill, containers, and balls of partially stabilized zirconia) and ultimately sintered at 1473 K with isothermal conditioning for 10 h in air. Submicron powders of LSGMC and SSC were synthesized using a similar technique. X-ray diffraction (XRD) patterns were registered at the room temperature using a Siemens D-500-Braun X02-1787 diffractometer ($\text{CuK}_{\alpha 1}$ -radiation, the step was 0.02° , the angle range was $20^\circ \leq 2\theta \leq 90^\circ$). X-ray patterns were processed and unit cell parameters were determined using the PowderCell software package (version 2.4).

Ceramic samples for measurement of specific conductivity were made using the obtained LSTM powders by the hydraulic compaction technique (~ 100 MPa) with the further sintering at 1723 K for 30 h in air. Conductivity was measured by a standard dc four-probe technique using ceramic plates with the size of $22 \times 3 \times 1.5$ mm³. Current electrodes made of platinum-based electrode paste were supported onto sample faces after purification in a sonication bath in ethanol. Platinum wires were used for manufacturing potential pressure electrodes. In the course of measurements, the sample was placed into oxidative and reducing atmospheres consisting of 80% nitrogen and 20% oxygen or 80% nitrogen and 20% hydrogen, accordingly. The sample temperature was maintained to the accuracy of ± 1 K. Conductivity measurements were carried out in the temperature range of 673–1073 K. The conductivity value was determined from the slope of the voltammetric characteristic measured at a constant temperature.

Chemical stability of LSTM towards the LSGMC solid electrolyte was estimated using the technique of powder mixture contact sintering at the mass ratio of 1 : 1 at 1623 K in air.

Studies of powder morphology and structure of electrodes, ceramic samples, and model fuel cells was carried out using a scanning electron microscope with a LEO SUPRA 50VP field emitting cathode at the accelerating voltages of 5–10 kV.

A planar SOFC design with a supporting solid electrolyte membrane was used for electrochemical studies. Laboratory SOFC samples represented high-density disks of anion LSGMC conductor (diameter, 20 mm, thickness, 0.5 mm) with porous anode and cathode layers. Anode and cathode powders were mixed with the Heraeus V-006 binder at the mass ratio of 1 : 1 and were consistently applied onto LSGMC disks using the screen-printing technique with the further sintering at 1573 K (for anodes) and at 1473 K (for cathodes). Measurements were carried out in a two-chamber test bench at 1173 K. The gas supplied to the anode was a mixture of H_2 (50 mL/min) and N_2 (50 mL/min). On the cathode side, the mixture of O_2 (50 mL/min) and N_2 (50 mL/min) was supplied. The gas flow rate was regulated using Bronkhorst controllers. The techniques and equipment for tests for model SOFC were described in detail earlier in [14].

RESULTS AND DISCUSSION

According to the data of XRD analysis, LSTM powders obtained in air at 1473 K were single-phase and had a structure of rhombohedrally distorted perovskite with space groups $R\bar{3}c$ (table). Unit cell parameters grew consistently at an increase in the content of lanthanum (table) which resulted in a decrease in the average degree of oxidation of manganese cations and therefore an increase in their radius.

One of the key requirements imposed on anodic SOFC materials is thermodynamic stability under oxidative conditions (in the course of synthesis and supporting on solid electrolyte membranes) and in reducing gas mixtures supplied to the anode in the course of operation of SOFC. In the latter case, application of partially converted hydrocarbon fuels was generally related to the presence of sulfur-containing admixtures that should not result in the poisoning of porous anodes at least due to kinetic causes. In stability tests, LSTM powders manufactured in air were subjected to heat treatment in a mixture of 80% N_2 –20% H_2 at 973–1073 K. In one case, gas flows were a pure mixture of N_2 and H_2 , in another, 5 ppm H_2S were additionally introduced into the atmosphere. Figures 1 and 2 show examples of XRD patterns for $\text{La}_{0.5}\text{Sr}_{0.5}\text{Mn}_{0.5}\text{Ti}_{0.5}\text{O}_{3-\delta}$ stoichiometric by *A*-sublattice and cation-deficient $(\text{La}_{0.6}\text{Sr}_{0.4})_{0.97}\text{Mn}_{0.5}\text{Ti}_{0.5}\text{O}_{3-\delta}$ after sintering under different conditions. In all cases, no formation of new phases as a result of reduction and reaction with H_2S is observed; the perovskite structure is preserved. However, the radius of cations of *B*-sublattice grows under reducing conditions (apart from partial reduction of Ti^{4+} to Ti^{3+} , the predominant part of Mn^{4+} ions is

Unit cell parameters and space groups of $(\text{La}_{0.5+x}\text{Sr}_{0.5-x})_{1-y}\text{Mn}_{0.5}\text{Ti}_{0.5}\text{O}_{3-\delta}$ after heat treatment under oxidative and reducing conditions

Composition	Heat treatment conditions	
	air, 1473 K*	80% N ₂ –20% H ₂ , 973 K**
$\text{La}_{0.5}\text{Sr}_{0.5}\text{Mn}_{0.5}\text{Ti}_{0.5}\text{O}_{3-\delta}$	$R\bar{3}c$ $a = 0.5517(2)$ nm, $\alpha = 60.130(3)^\circ$	$R\bar{3}c$ $a = 0.5551(2)$ nm, $a = 60.136(2)^\circ$
$\text{La}_{0.6}\text{Sr}_{0.4}\text{Mn}_{0.5}\text{Ti}_{0.5}\text{O}_{3-\delta}$	$R\bar{3}c$ $a = 0.5519(2)$ nm, $\alpha = 60.175(3)^\circ$	$R\bar{3}c$ $a = 0.5569(2)$ nm, $a = 59.887(3)^\circ$
$(\text{La}_{0.6}\text{Sr}_{0.4})_{0.97}\text{Mn}_{0.5}\text{Ti}_{0.5}\text{O}_{3-\delta}$	$R\bar{3}c$ $a = 0.5518(2)$ nm, $\alpha = 60.296(2)^\circ$	$Pnma$ $a = 0.5563(2)$ nm, $b = 0.7875(3)$ nm, $c = 0.5579(2)$ nm
$(\text{La}_{0.75}\text{Sr}_{0.25})_{0.97}\text{Mn}_{0.5}\text{Ti}_{0.5}\text{O}_{3-\delta}$	$R\bar{3}c$ $a = 0.5522(4)$ nm, $\alpha = 60.283(4)^\circ$	$Pnma$ $a = 0.5600(2)$ nm, $b = 0.7901(3)$ nm, $c = 0.5603(2)$ nm

* The heat treatment duration is 10 h, the heating rate is 150 K/h, natural cooling.

** The heat treatment duration is 5 h, the heating rate is 200 K/h, natural cooling.

reduced to Mn^{3+} and Mn^{2+}). The amount of oxygen producing a contracting effect on the structure becomes lower in reducing media. As a result, unit cell parameters increase in solid solutions stoichiometric by the *A*-sublattice (table). Compounds with deficiency by *A*-positions are also characterized by transition from a rhombohedral structure to an orthorhombically distorted perovskite one (space group *Pnma*). This trend is explained by changes in the Goldschmidt tolerance factor [15]; its decrease as a result of nonstoichiometry of the *A*-sublattice results in a decrease in

the crystal lattice symmetry. A similar effect is caused by an increase in the average radius of cations of the *B*-sublattice as a result of reduction. The volume of a LSTM pseudocubic unit cell increases by 1.8–4.1% under reduction. The perovskite structure is also preserved after the resintering of the reduced materials in air; herewith, the reverse transition from the orthorhombic modification to a rhombohedral one is observed for cation-deficient solid solutions (Fig. 2).

To estimate stability of LSTM at elevated temperatures, an additional series of samples was sintered in

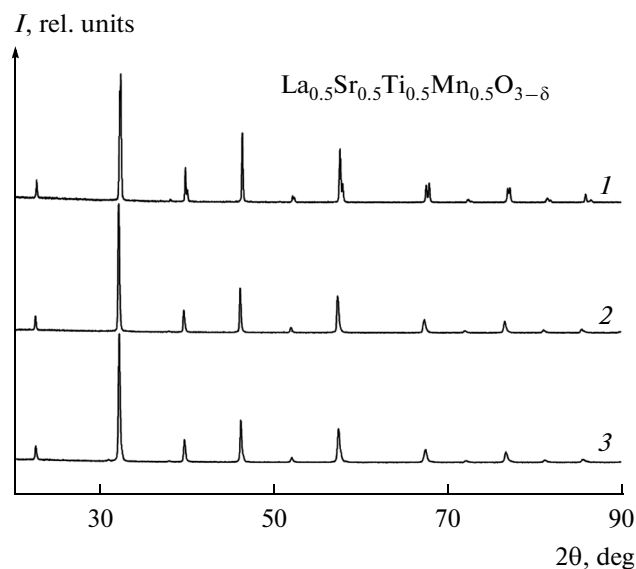


Fig. 1. XRD patterns of $\text{La}_{0.5}\text{Sr}_{0.5}\text{Ti}_{0.5}\text{Mn}_{0.5}\text{O}_{3-\delta}$: (1) obtained in air at 1473 K, (2) sintered in 80% N₂–20% H₂ at 973 K, (3) sintered in a flow of 80% N₂–20% H₂ in the presence of 5 ppm H₂S at 1073 K.

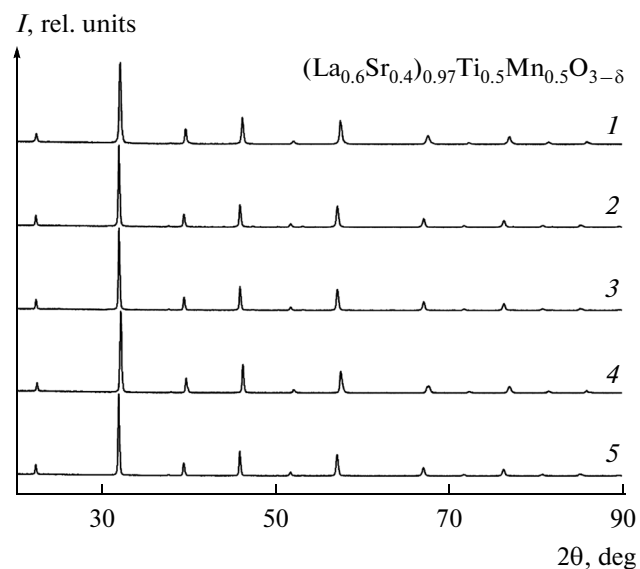


Fig. 2. XRD patterns of $(\text{La}_{0.6}\text{Sr}_{0.4})_{0.97}\text{Ti}_{0.5}\text{Mn}_{0.5}\text{O}_{3-\delta}$: (1) obtained in air at 1473 K, (2) sintered in 95% Ar–5% H₂ at 1473 K, (3) sintered in 80% N₂–20% H₂ at 973 K, (4) sintered in air at 1473 K after sintering in 80% N₂–20% H₂ at 973 K, (5) sintered in a flow of 80% N₂–20% H₂ in the presence of 5 ppm H₂S at 1073 K.

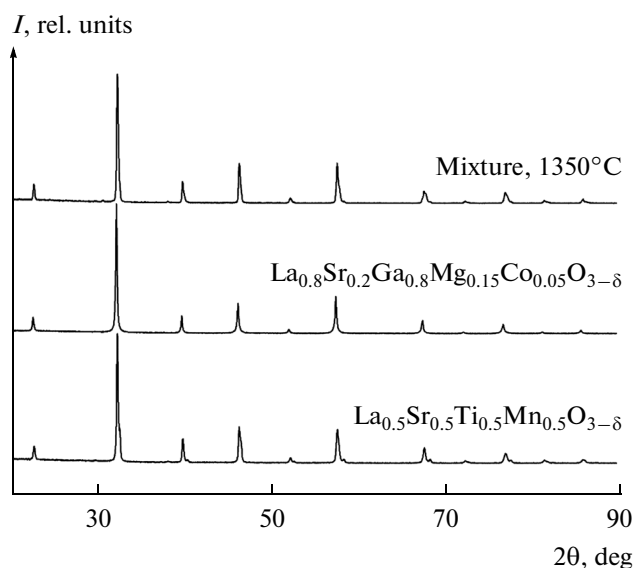


Fig. 3. XRD patterns of initial $\text{La}_{0.5}\text{Sr}_{0.5}\text{Ti}_{0.5}\text{Mn}_{0.5}\text{O}_{3-\delta}$ and LSGMC and their mixture sintered at 1623 K.

the flow of a gas mixture of 5% H_2 –95% Ar at 1473 K with conditioning for 3 h. For stoichiometric LSTM, partial decomposition was observed under these conditions with formation of ~13% LaSrMnO_4 tetragonal phase. The perovskite structure of cation-deficient LSTM was preserved (Fig. 2). Thus, 3% cation nonstoichiometry by the A-sublattice ($y = 0.03$) provides an increase in the phase stability of perovskite-like solid solutions at high reduction temperatures.

Another important criterion of applicability of SOFC anode materials is chemical stability in contact with the chosen solid electrolyte at elevated temperatures required for formation of electrochemical cells and electrode sintering. Figure 3 shows XRD patterns of $\text{La}_{0.5}\text{Sr}_{0.5}\text{Ti}_{0.5}\text{Mn}_{0.5}\text{O}_{3-\delta}$, LSGMC electrolyte, and their mixture (1 : 1) sintered at 1623 K. All reflexes belong to individual components of $\text{La}_{0.5}\text{Sr}_{0.5}\text{Ti}_{0.5}\text{Mn}_{0.5}\text{O}_{3-\delta}$ and LSGMC; no new phases are registered after the sintering of the mixture. Similar results were also obtained for the other system compositions.

Electron microscopy studies showed that the synthesized powders are homogeneous and have a rather narrow size distribution of grains (Fig. 4a). Powders consist of partially faceted particles with the size of 100–250 nm (Fig. 4b) that form agglomerates with the size of up to 400–500 nm (Fig. 4b). Such sizes are close to the optimum for the manufacturing of SOFC anodes, as a decrease in the grain size to tens of nm leads to considerable contraction under the electrode layer sintering, while excessive grain growth is related to a decrease in the surface area of the electrode and electrochemical reaction zone near the electrode/electrolyte interface.

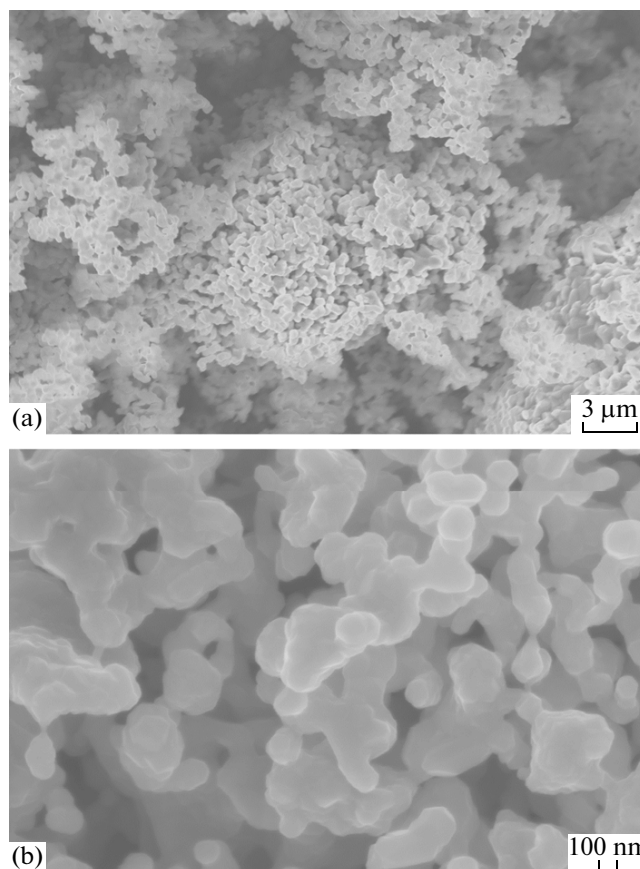


Fig. 4. (a, b) Microstructure of the $\text{La}_{0.5}\text{Sr}_{0.5}\text{Ti}_{0.5}\text{Mn}_{0.5}\text{O}_{3-\delta}$ electrode materials synthesized at 1473 K.

Figure 5 shows microphotographs of (a) the cross-section of the interface between the electrode and supporting electrolyte of the model SOFC and (b) the surface of an anode with the composition of $(\text{La}_{0.6}\text{Sr}_{0.4})_{0.97}\text{Mn}_{0.5}\text{Ti}_{0.5}\text{O}_{3-\delta}$ sintered at 1573 K. Such anode layers with the thickness of ~25 μm were characterized by good adhesion to gastight solid electrolyte membrane and a sufficiently developed specific surface. No traces of diffusion layer formation between the anode and electrolyte were observed. The size of grain particles of the $(\text{La}_{0.6}\text{Sr}_{0.4})_{0.97}\text{Mn}_{0.5}\text{Ti}_{0.5}\text{O}_{3-\delta}$ supported electrode was 100–500 nm. As LSTM and LSGMC are chemically compatible under the electrode sintering conditions, no buffer sublayers for model SOFC were used.

Temperature dependences of specific conductivity of ceramic LSTM samples in oxidative and reducing atmospheres are shown in Figs. 6a, 6b. Conductivity is well described within the standard Arrhenius model; activation energies are in the ranges of 0.21–0.25 eV in the atmosphere of 80% N_2 –20% O_2 and 0.21–0.52 eV in the flow of 80% N_2 –20% H_2 . The highest conductivity in an oxidative medium is characteristic of the composition of $\text{La}_{0.5}\text{Sr}_{0.5}\text{Ti}_{0.5}\text{Mn}_{0.5}\text{O}_{3-\delta}$, that in the reduc-

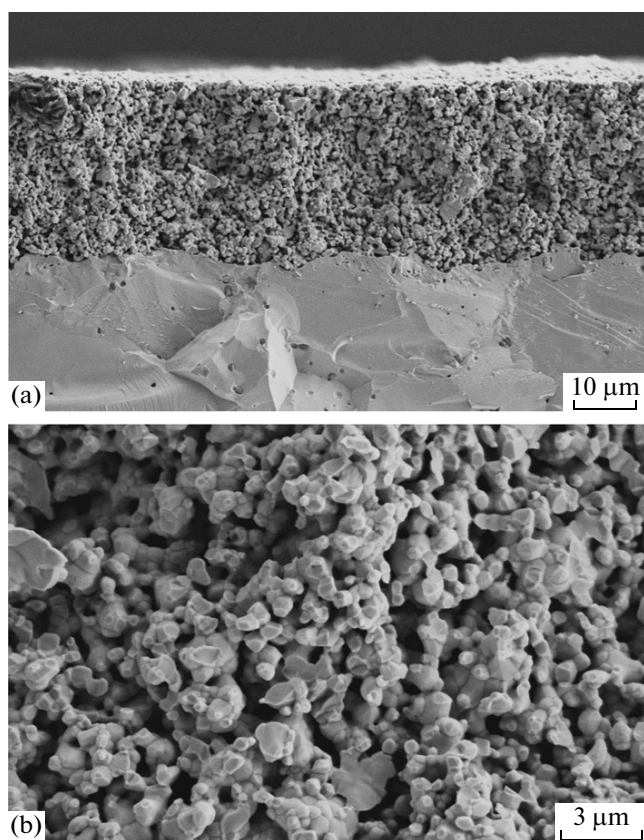


Fig. 5. (a, b) Electron microscopy images of (a) a cross-section of SOFC with supporting LSGMC electrolyte and a porous anode of $(\text{La}_{0.6}\text{Sr}_{0.4})_{0.97}\text{Ti}_{0.5}\text{Mn}_{0.5}\text{O}_{3-\delta}$ sintered at 1573 K and (b) the surface of this anode.

ing medium is typical for $(\text{La}_{0.6}\text{Sr}_{0.4})_{0.97}\text{Mn}_{0.5}\text{Ti}_{0.5}\text{O}_{3-\delta}$. Transition to the reducing atmosphere results in a considerable decrease in electron transport due to a decrease in the concentration of p -type charge carriers that dominate in perovskites of this system [6, 8]. Conductivity of LSTMs with stability in reducing media achieved by intercalation of $\text{Ti}^{4+/3+}$ cations is considerably lower than that of lanthanum-strontium manganites without substitution by the B -sublattice [16]. However, manganites are decomposed in a moderately reducing medium at relatively high chemical potentials of oxygen and cannot be used under anodic conditions. A decrease in conductivity in the case of LSTMs occurs as a result of intercalation of titanium cations forming stable Ti^{4+} states in oxidative atmospheres and the $\text{Ti}^{4+}/\text{Ti}^{3+}$ redox couple under reduction. Stability of these states is considerably higher as compared to $\text{Mn}^{4+}/\text{Mn}^{3+}$ and $\text{Mn}^{3+}/\text{Mn}^{2+}$ [17] existing in oxidized and partially reduced manganites. Accordingly, titanium cations under the studied conditions are largely excluded from the processes of hole migration and charge transport depends on the concentration of the $\text{Mn}^{4+}/\text{Mn}^{3+}$ and $\text{Mn}^{3+}/\text{Mn}^{2+}$

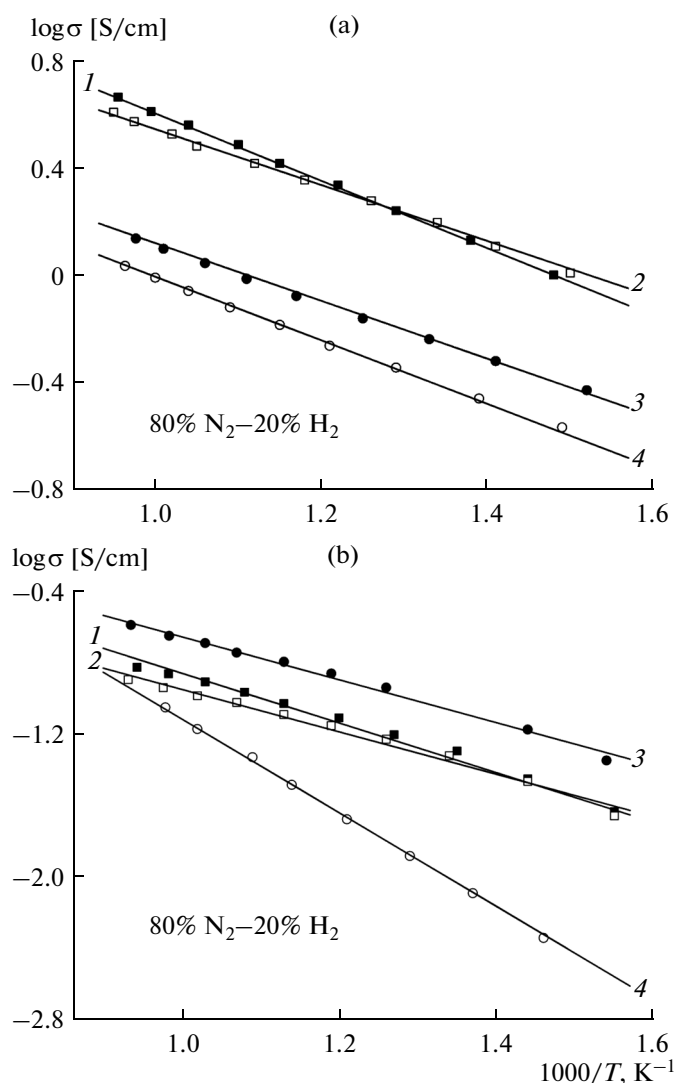


Fig. 6. Temperature dependences of conductivity of anodic materials: (a) in 80% N_2 –20% O_2 ; (b) in a flow of 80% N_2 –20% H_2 : (1) $\text{La}_{0.5}\text{Sr}_{0.5}\text{Ti}_{0.5}\text{Mn}_{0.5}\text{O}_{3-\delta}$, (2) $\text{La}_{0.6}\text{Sr}_{0.4}\text{Ti}_{0.5}\text{Mn}_{0.5}\text{O}_{3-\delta}$, (3) $(\text{La}_{0.6}\text{Sr}_{0.4})_{0.97}\text{Ti}_{0.5}\text{Mn}_{0.5}\text{O}_{3-\delta}$, (4) $(\text{La}_{0.75}\text{Sr}_{0.25})_{0.97}\text{Ti}_{0.5}\text{Mn}_{0.5}\text{O}_{3-\delta}$.

redox couples; their concentration in LSTMs is lower than in manganites under similar conditions. Besides, for electroneutrality, intercalation of Ti^{4+} is compensated by the further decrease in the concentration of Mn^{4+} . The latter effect is also obvious at an increase in the content of La^{3+} that causes a decrease in the concentration of Mn^{4+} and accordingly a decrease in conductivity under oxidative conditions (Fig. 6a).

Figure 7 shows voltammetric and power characteristics of laboratory SOFC with LSTMs-based anodes. Voltammetric curves at low and intermediate current densities contain no nonlinearities characteristic for Ni-cermet anodes as a result of oxidation of nickel. For SOFC with anodes of $(\text{La}_{0.6}\text{Sr}_{0.4})_{0.97}\text{Ti}_{0.5}\text{Mn}_{0.5}\text{O}_{3-\delta}$

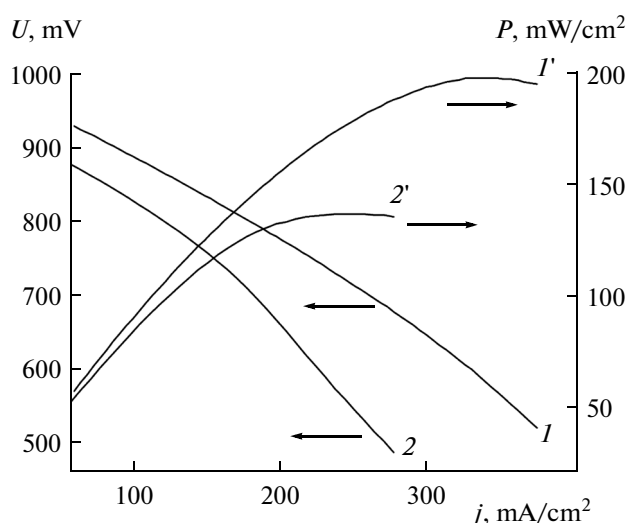


Fig. 7. Voltammetric and power characteristics of model fuel cells at 1173 K: (I, I') $(\text{La}_{0.6}\text{Sr}_{0.4})_{0.97}\text{Ti}_{0.5}\text{Mn}_{0.5}\text{O}_{3-\delta}$, ($2, 2'$) $(\text{La}_{0.75}\text{Sr}_{0.25})_{0.97}\text{Ti}_{0.5}\text{Mn}_{0.5}\text{O}_{3-\delta}$.

and $(\text{La}_{0.75}\text{Sr}_{0.25})_{0.97}\text{Ti}_{0.5}\text{Mn}_{0.5}\text{O}_{3-\delta}$, a linear region is observed at the currents of up to $\sim 180 \text{ mA/cm}^2$. The further increase in current density leads to an increase in the role of electrode polarization. The maxima of power density at 1173 K were 137 mW/cm^2 for the $(\text{La}_{0.75}\text{Sr}_{0.25})_{0.97}\text{Ti}_{0.5}\text{Mn}_{0.5}\text{O}_{3-\delta}$ anode and 198 mW/cm^2 for $(\text{La}_{0.6}\text{Sr}_{0.4})_{0.97}\text{Ti}_{0.5}\text{Mn}_{0.5}\text{O}_{3-\delta}$, which correlates with the electron conductivity level. The latter observation confirms the conclusion [6, 8, 9] that electrochemical activity of electrode materials of these groups is considerably limited by the electron transport processes. Characteristics of LSTM anodes are inferior to those of Ni–cermet anodes [18, 19] due to the lower conductivity and catalytic activity of manganites–titanates as compared to metallic nickel. However, redox stability of LSTM, comparatively lower reactivity in contact with lanthanum gallate, and absence of degradation in H_2S -containing atmospheres provide practically important advantages. The obtained characteristics of LSTM anodes are comparable with those of many well-known oxide anodic materials [20]. Therefore, the further optimization requires an increase in electron conductivity and addition of catalytically active centers. This problem can be solved by formation of a layer of nanosize particles of conducting materials with high catalytic activity (e.g., cerium oxide modified by microamounts of noble metals) on the surface of a sintered highly porous LSMT layer.

CONCLUSIONS

Single-phase submicron powders, ceramic, and porous anodes based on complex oxides with a perovs-

kite-like structure, with the general formula of $(\text{La}_{0.5+x}\text{Sr}_{0.5-x})_{1-y}\text{Mn}_{0.5}\text{Ti}_{0.5}\text{O}_{3-\delta}$ ($x = 0-0.25$, $y = 0-0.03$) were obtained in this work. XRD analysis showed that the obtained compounds are crystallized in air in the rhombohedral crystallographic system (space group $R\bar{3}c$). They are stable in a reducing atmosphere (20% $\text{H}_2-80\% \text{N}_2$) and in the presence of an admixture of hydrogen sulfide (5 ppm H_2S), and are chemically stable in contact with the solid electrolyte of $\text{La}_{0.8}\text{Sr}_{0.2}\text{Ga}_{0.8}\text{Mg}_{0.15}\text{Co}_{0.05}\text{O}_{3-\delta}$. Transition to a reducing atmosphere results in a considerable decrease in conductivity due to a decrease in the concentration of p -type electron charge carriers. Here-with, the highest conductivity in an oxidative medium is characteristic of the composition of $\text{La}_{0.5}\text{Sr}_{0.5}\text{Mn}_{0.5}\text{Ti}_{0.5}\text{O}_{3-\delta}$ and that in the reducing medium is typical for $(\text{La}_{0.6}\text{Sr}_{0.4})_{0.97}\text{Ti}_{0.5}\text{Mn}_{0.5}\text{O}_{3-\delta}$. Electrochemical tests of model SOFCs on the supporting electrolyte of $\text{La}_{0.8}\text{Sr}_{0.2}\text{Ga}_{0.8}\text{Mg}_{0.15}\text{Co}_{0.05}\text{O}_{3-\delta}$, with anodes based on $(\text{La}_{0.75}\text{Sr}_{0.25})_{0.97}\text{Ti}_{0.5}\text{Mn}_{0.5}\text{O}_{3-\delta}$ and $(\text{La}_{0.6}\text{Sr}_{0.4})_{0.97}\text{Ti}_{0.5}\text{Mn}_{0.5}\text{O}_{3-\delta}$ and a cathode of $\text{Sm}_{0.5}\text{Sr}_{0.5}\text{CoO}_{3-\delta}$ were carried out. The power density maximum was 198 mW/cm^2 . Functional properties of $(\text{La}_{0.5+x}\text{Sr}_{0.5-x})_{1-y}\text{Mn}_{0.5}\text{Ti}_{0.5}\text{O}_{3-\delta}$ allow developing porous anodic layers based on these materials.

ACKNOWLEDGMENTS

The work was financially supported by the Ministry of Education and Science of the Russian Federation (Contracts 02.740.11.5214 and 14.V25.31.0018).

REFERENCES

1. Ishihara, T., Tabuchi, J., Ishikawa, S., Yan, J., Enoki, M., and Matsumoto, H., *Solid State Ionics*, 2006, vol. 177, nos. 19–25, p. 1949.
2. Choi, J.-J., Cho, K.-S., Choi, J.-H., Ryu, J., Hahn, B.-D., Yoon, W.-H., Kim, J.-W., Ahn, C.-W., Park, D.-S., and Yun, J., *Int. J. Hydrogen Energy*, 2012, vol. 37, no. 8, p. 6830.
3. Kim, K.N., Kim, B.K., Son, J.W., Kim, J., Lee, H.-W., Lee, J.-H., and Moon, J., *Solid State Ionics*, 2006, vol. 177, nos. 19–25, p. 2155.
4. Somalu, M.R., Yufit, V., Cumming, D., Lorente, E., and Brandon, N.P., *Int. J. Hydrogen Energy*, 2012, vol. 36, no. 9, p. 5557.
5. Kuhn, J.N., Lakshminarayanan, N., and Ozkan, U.S., *J. Mol. Catal. A: Chem.*, 2008, vol. 282, nos. 1–2, p. 9.
6. Kolotygin, V.A., Tsipis, E.V., Shaula, A.L., Naumovich, E.N., Frade, J.R., Bredikhin, S.I., and Kharton, V.V., *J. Solid State Electrochem.*, 2011, vol. 15, no. 2, p. 313.
7. Kim, J.H., Schlegel, H., and Irvine, J.T.S., *Int. J. Hydrogen Energy*, 2012, vol. 37, no. 19, p. 14511.
8. Kolotygin, V.A., Tsipis, E.V., Ivanov, A.I., Fedotov, Y.A., Burmistrov, I.N., Agarkov, D.A., Sinitsyn, V.V.,

- Bredikhin, S.I., and Kharton, V.V., *J. Solid State Electrochem.*, 2012, vol. 16, no. 7, p. 2335.
9. Kolotygin, V.A., Tsipis, E.V., Lu, M.F., Pivak, Y.V., Yarmolenko, S.N., Bredikhin, S.I., Kharton, V.V., *Solid State Ionics*, 2014, vol. 260, p. 15.
 10. Ovalle, A., Ruiz-Morales, J.C., Canales-Vázquez, J., Marrero-López, D., and Irvine, J.T.S., *Solid State Ionics*, 2006, vol. 177, nos. 19–25, p. 1997.
 11. Choi, J.-J., Cho, K.-S., Choi, J.-H., Ryu, J., Hahn, B.-D., Yoon, W.-H., Kim, J.-W., Ahn, C.-W., Park, D.-S., and Yun, J., *Int. J. Hydrogen Energy*, 2012, vol. 37, no. 8, p. 6830.
 12. Perovskite Oxide for Solid Oxide Fuel Cells, Ishihara, T., Ed., Springer, 2009.
 13. Pechini, M., US Patent 330697, 1967.
 14. Burmistrov, I.N., *Cand. Sci. (Phys.-Math.) Dissertation*, Chernogolovka: IFTT RAN, 2010.
 15. Urusov, V.S., *Teoreticheskaya kristalokhimiya* (Theoretical Crystallochemistry), Moscow: Izd-vo MGU, 1987.
 16. Jiang, S.P., *J. Mater. Sci.*, 2008, vol. 43, no. 21, p. 6799.
 17. Samsonov, G.V., *Fiziko-khimicheskie svoistva okislov* (Physico-Chemical Properties of Oxides), Moscow: Metallurgiya, 1978.
 18. Hwang, C., Tsai, C.-H., Lo, C.-H., and Sun, C.-H., *J. Power Sources*, 2008, vol. 180, no. 1, p. 132.
 19. Hong, J.-E., Inagaki, T., Ida, S., and Ishihara, T., *Int. J. Hydrogen Energy*, 2011, vol. 36, no. 22, p. 14632.
 20. Tsipis, E.V. and Kharton, V.V., *J. Solid State Electrochem.*, 2011, vol. 15, no. 5, p. 1007.

Translated by M. Ehrenburg